Emergency Radiology (2020) 27:701–710
https://doi.org/10.1007/s10140-020-01867-1

ORIGINAL ARTICLE

Qualitative and quantitative chest CT parameters as predictors of specific mortality in COVID-19 patients

Davide Colombi[1] · Gabriele D. Villani[1] · Gabriele Maffi[1] · Camilla Risoli[1] · Flavio C. Bodini[1] · Marcello Petrini[1] · Nicola Morelli[1] · Pietro Anselmi[1] · Gianluca Milanese[2] · Mario Silva[2] · Nicola Sverzellati[2] · Emanuele Michieletti[1]

Received: 2 September 2020 / Accepted: 23 October 2020 / Published online: 29 October 2020

Abstract

Purpose To test the association between death and both qualitative and quantitative CT parameters obtained visually and by software in coronavirus disease (COVID-19) early outbreak.

Methods The study analyzed retrospectively patients underwent chest CT at hospital admission for COVID-19 pneumonia suspicion, between February 21 and March 6, 2020. CT was performed in case of hypoxemia or moderate-to-severe dyspnea. CT scans were analyzed for quantitative and qualitative features obtained visually and by software. Cox proportional hazards regression analysis examined the association between variables and overall survival (OS). Three models were built for stratification of mortality risk: clinical, clinical/visual CT evaluation, and clinical/software-based CT assessment. AUC for each model was used to assess performance in predicting death.

Results The study included 248 patients (70% males, median age 68 years). Death occurred in 78/248 (32%) patients. Visual pneumonia extent > 40% (HR 2.15, 95% CI 1.2–3.85, $P = 0.01$), %high attenuation area – 700 HU > 35% (HR 2.17, 95% CI 1.2–3.94, $P = 0.01$), exudative consolidations (HR 2.85–2.93, 95% CI 1.61–5.05/1.66–5.16, $P < 0.001$), visual CAC score > 1 (HR 2.76–3.32, 95% CI 1.4–5.45/1.71–6.46, $P < 0.01$/$P < 0.001$), and CT classified as COVID-19 and other disease (HR 1.92–2.03, 95% CI 1.01–3.67/1.06–3.9, $P = 0.04$/$P = 0.03$) were significantly associated with shorter OS. Models including CT parameters (AUC 0.911–0.913, 95% CI 0.873–0.95/0.875–0.952) were better predictors of death as compared to clinical model (AUC 0.869, 95% CI 0.816–0.922; $P = 0.04$ for both models).

Conclusions In COVID-19 patients, qualitative and quantitative chest CT parameters obtained visually or by software are predictors of mortality. Predictive models including CT metrics were better predictors of death in comparison to clinical model.

Keywords COVID-19 · CT scan · Survival analysis · Computer Software Applications

Introduction

Severe acute respiratory syndrome coronavirus 2 (SARS-CoV-2) and the related coronavirus disease 2019 (COVID-19) were described for the first time in Wuhan, China, in December 2019 [1]. The pandemic evolution of SARS-CoV-2 reached over 20 million cases and over 700,000 deaths worldwide, by August 2020 [2]. Several comorbidities and clinical conditions have been investigated and proposed for triaging and stratify risk of death in COVID-19 [3]. Also radiology plays a relevant role for the risk stratification in patients with suspected COVID-19 pneumonia, notably the scientific debate showed that both chest radiography and computed tomography (CT) could contribute in the management of patients. During the first wave, the use of radiology was quite heterogenous; in particular, it was managed according to local organization in radiology departments and, utmost, in clinical and laboratory capacity. The use of CT led to understanding that visual quantification of COVID-19 pneumonia extent and several features (predominant crazy-paving pattern

Supplementary Information The online version contains supplementary material available at https://doi.org/10.1007/s10140-020-01867-1.

✉ Davide Colombi
D.Colombi@ausl.pc.it

[1] Department of Radiological Functions, Radiology Unit, "Guglielmo da Saliceto" Hospital, Via Taverna 49, 29121 Piacenza, Italy

[2] Department of Medicine and Surgery (DiMeC), Unit "Scienze Radiologiche", University of Parma, Padiglione Barbieri, V. Gramsci 14, Parma, Italy

or presence of consolidations) at chest CT are associated with increased risk of death [4–6]. In addition, CT quantitative parameters obtained by software predict the severity of COVID-19 pneumonia and its progression [7, 8].

The purpose of the present study was to describe both qualitative and quantitative CT parameters obtained visually and by an open-source software in COVID-19 pneumonia and test their association with survival.

Materials and methods

Study population

This retrospective study was approved by the Local Ethics Committee (institutional review board -IRB- approval number 582/2020/OSS*/AUSLPC). The informed consent was waived by the IRB due to the retrospective nature of the study. The study included consecutive patients that underwent chest CT at the emergency department admission in suspicion of COVID-19 pneumonia, in the time interval February 21 to March 6, 2020. Considering the environment of high community disease burden and the unavailability of rapid point-of-care COVID-19 testing, CT was used in the work up of patients presenting with clinical moderate-to-severe features (e.g., hypoxemia, moderate-to-severe dyspnea) consistent with COVID-19 infection [9]. All the patients performed reverse-transcription polymerase chain reaction (RT-PCR) for SARS-CoV-2 in nasal-pharyngeal swabs. In cases of negative RT-PCR results and persistent clinical suspicion of COVID-19, the patients were retested within 48 h. Patients with at least one positive RT-PCR within 48 h from casualty admission were included in the study. Patients with only a single negative RT-PCR swab and positive serum IgG title anti-SARS-CoV-2 (Abbott SARS-CoV-2 IgG; Abbott Diagnostics, IL, USA) based on the chemiluminescence enzyme immunoassays (CLIA) performed > 14 days after symptoms onset were also included in the study. Patients with double negative result of RT-PCR for SARS-CoV-2 in swabs were excluded from the study. Patient enrollment process is showed in Fig. 1. Two hundred and thirty-six patients of this population were analyzed in a previous study [10].

Epidemiological data, comorbidities, symptoms, laboratory findings, and diagnostic imaging test performed with the corresponding results for each included patient were recorded at admission. CT was performed within 12 h from the clinical evaluation and laboratory testing.

CT protocol and image analysis

Chest CT protocol was showed in a previous study [10]. After each examination, the room was decontaminated by a solution at 62–71% of ethanol or 0.1% of sodium hypochlorite [11]. The scanner cleaning procedure required around 15–20 min for each patient.

Visual chest CT interpretation was independently performed by two radiologists (D.C. and G.D.V.) blinded to clinical data, respectively with 5 and 11 years of experience. Each observer identified the presence of ground-glass opacity (GGO), crazy-paving pattern (CP), and consolidation (CONS), as defined by the Fleischner Society Glossary of terms for Thoracic Imaging [12]. Consolidations were then classified as exudative, band-like, organizing, or as atelectasis [13]. The readers assessed the presence of emphysema (> 5% of overall pulmonary volume), pulmonary fibrosis, pleural effusion, mediastinal nodal enlargement (short-axis ≥ 10 mm), and hiatal hernia. The "fat vessel sign" was defined as a subsegmental vascular enlargement > 3 mm [14]. "Sparing of the central interstitium" was considered in patients with sparing of the parenchyma surrounding vessel and bronchi within more than 30% of pneumonia extent. Visual assessment of coronary artery calcium (CAC) was performed as proposed by Azour et al. [15]. The hepatic density was estimated by averaging the Hounsfield unit (HU) measure of three region of interest (ROI) in the VII, VIII, and II segment; the ratio of the hepatic density and splenic density (HU) was also calculated. Then the reader categorized CT findings as proposed by Sverzellati et al. (Online Resource 1) [16]. The total extent of COVID-19 pneumonia, the GGO and CP sum (GGO+CP), and CONS were expressed as percentage of total lung volume and estimated to the nearest 5% in three lung zones showed in a previous report and averaged to produce a global percentage of abnormalities extent [10, 17, 18]. The axial distribution was classified as peripheral (prevalent in the outer third of the lung) or central (predominant in the inner two-third). Consensus formulation for the visual scores and for categorical CT assessment was defined in previous study [10].

The software-based evaluation was performed on a dedicated workstation using the extension Chest Imaging Platform (Applied Chest Imaging Laboratory; Boston, MA, USA) of the open-source 3D Slicer software (version 4.10.2, https://www.slicer.org) [19]. A fully automatic lung segmentation and analysis of lung parenchyma histogram was obtained using B40f kernel (Fig. 2). A radiologist (D.C.) and a radiology technician (C.R.) both with 5 years of experience accomplished the segmentation of each patient and, if unsatisfactory, amended the lung contours with a manual tool. The time to obtain the software-based analysis and requirement of manual correction were recorded for each patient in both readers. The percentage of the total lung volume with attenuation higher (high attenuation area, HAA) than − 700 HU (%HAA − 700), − 600 HU (%HAA − 600), − 500 HU (%HAA − 500), and − 250 HU (%HAA − 250) were recorded; furthermore, were calculated the percentage of the lung volume included between − 700 and − 250 HU (%HAA − 700–250) or between

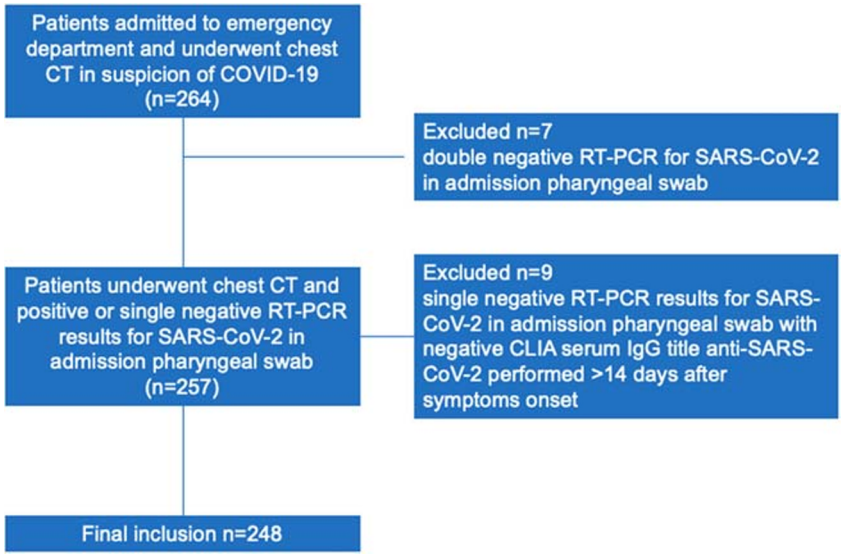

Fig. 1 The diagram shows the patient enrollment process. CLIA, chemiluminescence enzyme immunoassays; COVID-19, coronavirus disease 2019; CT, computed tomography; RT-PCR, reverse-transcription polymerase chain reaction; SARS-CoV-2, severe acute respiratory syndrome coronavirus 2

− 600 and − 250 HU (%HAA − 600–250). Percentage of low attenuation area (LAA) less than − 950 HU (%LAA − 950) was additionally provided. Histogram skewness and kurtosis were also analyzed.

Statistical analysis

Categorical and continuous variables were expressed as counts and percentage or median with corresponding 95% confidence interval (95% CI). Patients were categorized in two groups, survivors and non-survivors; the difference between groups was assessed by Mann-Whitney *U* test for continuous variables and chi-square test or Fisher's exact test for categorical variables, as appropriate. The Spearman coefficient of rank correlation (rho) was calculated to test the relationship between visual CT and software-based scores across the range of predefined density thresholds. The inter-rater agreement was tested with the intra-class correlation coefficient (ICC) and the weighted Cohen's kappa (K_w) [20]. The interpretation of ICC and of the K_w was based on previous guidelines [21, 22].

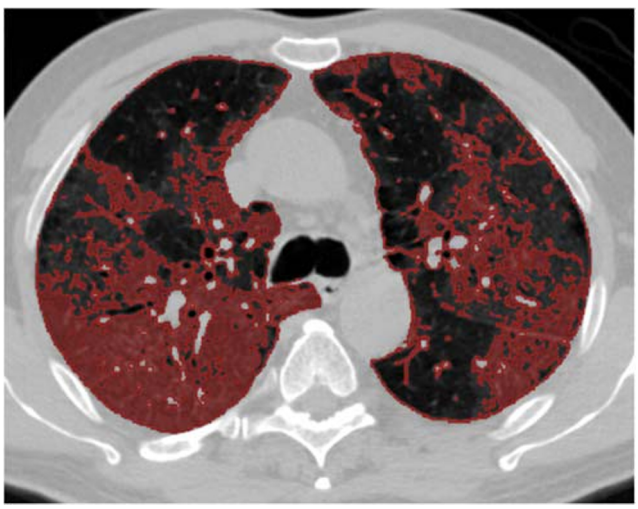

Fig. 2 A 70-year-old man admitted to the emergency department with cough and fever from 1 week, with positive RT-PCR nasal-pharyngeal swab for SARS-CoV-2, who died 13 days after hospital admission. The axial admission non-enhanced CT image at the level of carina after applying a density mask (between − 700 and − 250 HU) using an open-source software displays in red the sum of ground glass opacities and crazy paving pattern. CT, computed tomography; HU, Hounsfield unit; RT-PCR, reverse-transcription polymerase chain reaction; SARS-CoV-2, severe acute respiratory syndrome coronavirus 2

The overall survival (OS) was calculated from the date of the admission CT to the time of specific death for COVID-19, as defined by the World Health Organization (WHO) [23]. Variables significantly different between survivors and non-survivors with clinical or radiological impact were considered as potential predictors of death. Receiver operating characteristic (ROC) curve were calculated for potential predictors of specific death. The highest value of the Youden Index was obtained to determine an appropriate cutoff to transform continuous variables in binary categorical variables. Cox proportional hazards regression analysis was used to examine the association between prognostic variables and OS to estimate hazard ratios (HR) and 95% CI. At univariable analysis, potential predictors with P value < 0.1 were included in the multivariable analysis using a stepwise regression model. Therefore, was obtained a model using only demographics and clinical parameters; additional models were calculated by adding categories derived from qualitative and quantitative CT metrics assessed visually or by software. ROC curve analysis was performed for each model and the area under the ROC (AUC) was used to assess the performance of the discrimination models based on independent predictors. The ROC curves of the models were compared by the methodology of DeLong et al. [24]. Categories on the basis of potential prognostic variables were correlated with OS using the

Kaplan-Meier method (product-limit). The survival functions were compared between independent groups of patients by means of the log-rank test. A P value < 0.05 was considered significant. Statistical analysis was performed using MedCalc software (version 14.8.1, MedCalc Software Ltd, Ostend, Belgium).

Results

Patient characteristics

In Table 1 are summarized demographics, comorbidities, clinical, and laboratory findings.

In the period considered, 264 patients were tested for SARS-CoV-2 with nasal-pharyngeal swab. One swab was performed in 252/264 (95%, 95% CI 92–97%) patients, with positive result in 240/252 (95%, 95% CI 92–97%) cases. Of the remaining patients with single negative swab, 3/12 (25%, 95% CI 9–53%) showed positive serum IgG title anti-SARS-CoV-2 > 14 days after symptoms onset, while the remaining 9/12 (75%, 95% CI 47–91%) patients confirmed the negative swab result at serology. Double swab was obtained in 12/264 (5%, 95% CI 3–8%) patients. In 7/12 (58%, 95% CI 32–80%) cases, the result was double negative, while a positive swab was obtained within 48 h in the remaining 5/12 (42%, 95% CI 19–68%) patients.

Thus, the study included 248 patients, predominantly males (174/248, 70%, 95% CI 64–75%), with a median age of 68 years (95% CI 65–70 years). The group of survivors included 170/248 (68%, 95% CI 62–74%) patients, while death occurred in 78/248 (32%, 95% CI 26–37%) patients. Non-survivors had a higher rate of cardiovascular (74% vs 46%, P < 0.001), oncological (24% vs 8%, P < 0.001), and

Table 1 Patients demographics, comorbidities, symptoms, and main laboratory findings at admission

Variable	Total (n = 248)	Survivors (n = 170)	Non-survivors (n = 78)	P value
Age	68 (65–70)	62 (59–64)	77 (75–79)	< 0.001*
Gender				
• females	74 (30%, 24–35%)	50 (29%, 23–36%)	24 (31%, 21–41%)	0.94
Smoking history (unavailable 143/248 patients, 58%)				
• Non-smokers	64 (26%, 21–32%)	53 (31%, 25–38%)	11 (14%, 8–24%)	< 0.01*
• Former smokers	31 (12%, 9–17%	19 (11%, 7–17%)	12 (15%, 9–25%)	0.47
• Current smokers	10 (4%, 2–7%)	5 (3%, 1–7%)	5 (6%, 3–14%)	0.34
Exposure to subject with known COVID-19 infection	94 (38%, 32–44%)	72 (42%, 35–50%)	22 (28%, 19–39%)	0.04*
Comorbidity				
• Cardiovascular	136 (55%, 49–61%)	78 (46%, 39–53%)	58 (74%, 64–83%)	< 0.001*
• Pulmonary	37 (15%, 11–20%)	23 (14%, 9–19%)	14 (18%, 11–28%)	0.49
• Oncological	32 (13%, 9–18%)	13 (8%, 4–12%)	19 (24%, 16–35%)	< 0.001*
• Neurological	34 (14%, 10–19%)	10 (6%, 3–10%)	24 (31%, 22–42%)	< 0.001*
• Diabetes	45 (18%, 14–23%)	25 (15%, 10–20%)	20 (26%, 17–36%)	0.06
Symptom				
• Fever	239 (96%, 93–98%)	169 (99%, 97–100%)	70 (90%, 81–95%)	0.78
• Cough	154 (62%, 56–68%)	116 (68%, 61–75%)	38 (49%, 38–60%)	< 0.01*
• Dyspnea	114 (46%, 40–52%)	74 (44%, 36–51%)	40 (51%, 40–62%)	0.15
Symptoms onset (days)	7 (5–7)	7 (6–7)	4 (3–7)	< 0.01*
Respiratory rate (acts/min)	20 (18–20)	20 (18–22)	22 (20–25)	< 0.001*
Hemoglobin (g/dl)	13.8 (13.5–14.2)	14.2 (13.7–14.5)	13.1 (12.4–13.7)	< 0.001*
White blood cell count (× 10^3/μl)	6.3 (5.9–6.9)	5.9 (5.6–6.3)	8 (7–9.3)	< 0.001*
Lymphocytes (× 10^3/μl)	0.98 (0.93–1.03)	1.02 (0.97–1.11)	0.81 (0.76–0.99)	0.01*
Platelet (× 10^3/μl)	182 (173–191)	179 (168–191)	184 (171–217)	0.17
CRP (mg/dl)	8.4 (6.8–9.4)	6.3 (5.3–8.3)	13.4 (11.4–15.5)	< 0.001*
Blood urea level (mg/dl)	39 (37–45)	36 (33–38)	61 (55–64)	< 0.001*
GOT (U/l)	42 (38–45)	39 (36–43)	46 (42–58)	0.07
GPT (U/l)	32 (27–94)	33 (27–36)	28 (23–33)	0.05

Categorical and continuous variables are expressed as counts and percentage or median, with corresponding 95% confidence interval (95% CI) in parentheses. Significant P values are identified by asterisks

COVID-19, coronavirus disease 2019; *CRP*, C-reactive protein; *GOT*, glutamic oxaloacetic transaminase; *GPT*, glutamic pyruvic transaminase

neurological (31% vs 6%, $P < 0.001$) comorbidities. In comparison to non-survivors, patients who survived were younger (median age 62 vs 77 years, $P < 0.001$) and showed lower median value of C-reactive protein (CRP, 6.3 vs 13.4 mg/dl, $P < 0.001$) and white blood cell count (5.9 vs 8 x 10^3/μl, $P < 0.001$). Non-survivor patients had higher levels of blood urea (61 vs 36 mg/dl, $P < 0.001$). Lung ultrasound (LUS) was performed in 229/248 (92%, 95% CI 88–95%) patients; the majority (215/229, 94%, 95% CI 96–90%) considered positive for COVID-19 pneumonia. Among included patients, 52/248 (21%, 95% CI 16–26%) underwent chest x-ray, abnormal in 46/52 (88%, 95% CI 77–95%) cases.

Relationships and inter-reader agreement of visual and software-based CT assessment

The highest correlations (Online Resource 2) were found for the overall pneumonia extent with %HAA − 700 (rho 0.781, 95% CI 0.727–0.826, $P < 0.001$), for GGO+CP with %HAA − 700–250 (rho 0.612, 95% CI 0.527–0.685, $P < 0.001$), and for CONS with %HAA − 250 (rho 0.622, 95% CI 0.539–0.694, $P < 0.001$).

Online Resource 3 displays the inter-reader agreement results. Considering the visual assessment, the agreement was good for overall pneumonia extent (ICC 0.896, 95% CI 0.866–0.92), GGO+CP extent (ICC 0.816, 95% CI 0.764–0.857), and visual assessment of CAC (ICC 0.781, 95% CI 0.722–0.829) while it was excellent for CONS (ICC 0.901, 95% CI 0.871–0.923) extent. Reproducibility was good for COVID-19 CT categories (K_w 0.707, 95% CI 0.656–0.758) and consolidations assessment (K_w 0.63, 95% CI 0.556–0.711), while very good for pleural effusion (K_w 0.948, 95% CI 0.889–1). Nevertheless, the inter-reader agreement for sparing of the central interstitium and fat vessel sign was fair (respectively K_w 0.371, 95% CI 0.208–0.533; K_w 0.226, 95% CI 0.121–0.33). Inter-observer agreement of the software-based metrics was excellent for all metrics except for good reproducibility in %HAA − 250 (ICC 0.848, 95% CI 0.778–0.897). No significant differences between readers were found neither for the rate of manual correction (56% for the radiologist vs 65% for the technician, $P = 0.29$) nor for the time required to obtain the automatic lung segmentation (median time 226 s for the radiologist vs 264 s for the technician, $P = 0.28$).

Qualitative and quantitative CT findings

Table 2 summarizes CT findings. Non-survivors patients had a higher overall pneumonia extent (40% vs 25%, $P < 0.001$), GGO+CP extent (25% vs 16%, $P = 0.01$), CONS extent (7% vs 4%, $P = 0.01$), and visual score of CAC (3 vs 1, $P < 0.001$). Exudative consolidation (36% vs 18%, $P < 0.01$), pleural effusion (35% vs 15%, $P < 0.01$), and patients with CT categorized as COVID-19 and other disease (23% vs 3%, $P < 0.001$) were more frequent in non-survivors patients. In non-survivors patients with COVID-19 and other disease, the concomitant pathology was pulmonary edema in 12/18 (67%; 95% CI 44–84%) patients, while pneumonia other than COVID-19 in 6/18 (33%, 95% CI 16–56%) cases. The %HAA − 700 (40% vs 25%, $P < 0.001$), %HAA − 700–250 (32% vs 21%, $P < 0.001$), %HAA − 250 (6% vs 4%, $P < 0.001$), and %LAA − 950 (0.6 vs 0.46, $P = 0.04$) were more extended in non-survivors patients.

Survival analysis

The median observation time from admission CT was 75 days (95% CI 61–81 days). Online Resource 4 provided in supplementary materials shows the best cutoff obtained by the ROC curve analysis in relation to specific death. Cox proportional hazards regression analysis results are reported in Table 3. In the model containing clinical and CT variables derived by visual CT assessment, overall pneumonia extent > 40% (HR 2.15, 95% CI 1.2–3.85, $P = 0.01$), exudative consolidations (HR 2.93, 95% CI 1.66–5.16, $P < 0.001$), visual CAC score > 1 (HR 2.76, 95% CI 1.4–5.45, $P < 0.01$), and patients with CT classified as COVID-19 and other disease (HR 2.03, 95% CI 1.06–3.9, $P = 0.03$) were significantly associated with shorter survival. Accordingly with the previous model, in the additional model containing clinical and CT variables derived by both software-based and visual CT assessment, %HAA − 700 > 35% (HR 2.17, 95% CI 1.2–3.94, $P = 0.01$), exudative consolidations (HR 2.85, 95% CI 1.61–5.05, $P < 0.001$), visual CAC score > 1 (HR 3.32, 95% CI 1.71–6.46, $P < 0.001$), and patients with CT classified as COVID-19 and other disease (HR 1.92, 95% CI 1.01–3.67, $P = 0.04$) were significantly associated with shorter survival. Models with additional visual CT assessment (AUC 0.911, 95% CI 0.873–0.95) and visual plus software-based CT assessment (AUC 0.913, 95% CI 0.875–0.952) were similar ($P = 0.68$); nevertheless, models containing CT metrics showed a significant higher performance for death prediction as compared to the model containing only clinical variables (AUC 0.869, 95% CI 0.816–0.922; $P = 0.04$ for both models; Fig. 3). As displayed in Online Resource 5, significant shorter survival was found in patients with visual CT overall pneumonia extent > 40% (mean survival 55 vs 100 days, $P < 0.001$), %HAA − 700 > 35% (mean survival 60 vs 104 days, $P < 0.001$), exudative consolidations (mean survival 70 vs 94 days, $P < 0.01$), visual CAC score > 1 (mean survival 69 vs 107 days, $P < 0.001$), and CT category of COVID-19 and other disease (mean survival 33 vs 94 days, $P < 0.001$).

Discussion

This study demonstrated that the visual overall extent of interstitial pneumonia > 40% of the total lung volume, the %HAA

Table 2 Qualitative and quantitative computed tomography findings

Variable	Total (n = 248)	Survivors (n = 170)	Non-survivors (n = 78)	P value
Visual overall pneumonia extent (%)	30 (25–30)	25 (20–25)	40 (32–50)	< 0.001*
Visual ground glass and crazy paving opacities extent (%)	20 (16–22)	16 (14–20)	25 (21–37)	0.01*
Visual consolidations extent (%)	5 (4–6)	4 (2–4)	7 (5–13)	0.01*
Distribution				
• Diffuse	182 (73%, 67–78%)	121 (71%, 64–77%)	61 (78%, 68–86%)	0.31
• Central	8 (3%, 2–6%)	4 (2%, 0.9–6%)	4 (5%, 2–12%)	0.44
• Peripheral	55 (22%, 17–28%)	43 (25%, 19–32%)	12 (15%, 9–25%)	0.11
Consolidation type				
• Solid	60 (24%, 19–30%)	32 (18%, 14–25%)	28 (36%, 26–47%)	< 0.01*
• Band-like	62 (25%, 20–31)	53 (31%, 25–38%)	9 (11%, 6–21%)	< 0.01*
• Organizing type	24 (10%, 7–14%)	17 (10%, 6–15%)	7 (9%, 4–17%)	0.98
• Atelectasis	21 (8%, 6–13%)	11 (6%, 4–11%)	10 (13%, 7–22%)	0.15
Emphysema (> 5% at visual assessment)	44 (18%, 13–23%)	25 (15%, 10–21%)	19 (24%, 16–35%)	0.09
Fibrosis	8 (3%, 2–6%)	4 (2%, 0.9–6%)	4 (5%, 2–12%)	0.44
Pleural effusion	53 (21%, 17–27))	26 (15%, 11–21%)	27 (35%, 25–46%)	< 0.01*
Mediastinal node enlargement	56 (22%, 18–28%)	32 (19%, 14–25%)	24 (31%, 22–42%)	0.05
Fat vessel sign	100 (40%, 34–47%)	66 (39%, 32–46%)	34 (44%, 33–55%)	0.57
Sparing of central interstitium	42 (17%, 13–22%)	38 (22%, 17–29%)	4 (5%, 2–12%)	< 0.01*
Visual coronary artery calcium score	1.5 (1–2)	1 (1–1)	3 (2–4)	< 0.001*
Ratio hepatic/splenic density	2.4 (2.3–2.5)	2.4 (2.4–2.6)	2.4 (2.4–2.6)	0.72
Hiatal hernia	99 (40%, 34–46%)	66 (39%, 32–46%)	33 (42%, 32–53%)	0.7
CT categories for COVID-19				
• Negative	3 (1%, 0.4–4%)	2 (1%, 0.3–4%)	1 (1%, 0.2–7%)	0.57
• Indeterminate				
○ COVID-19 or other disease	12 (5%, 3–8%)	8 (5%, 2–9%)	4 (6%, 2–14%)	0.86
○ COVID-19 and other disease	23 (9%, 6–14%)	5 (3%, 1–7%)	18 (23%, 15–34%)	< 0.001*
• Typical	210 (85%, 80–89%)	155 (91%, 86–95%)	55 (70%, 60–79%)	< 0.001*
HAA − 700 HU (%)	30 (26–33)	25 (22–28)	40 (35–47)	< 0.001*
HAA − 250 HU (%)	4 (4–5)	4 (3–4)	6 (5–8)	< 0.001*
HAA − 700–250 HU (%)	24 (22–26)	21 (19–24)	32 (27–36)	< 0.001*
LAA − 950 HU (%)	0.51 (0.43–0.57)	0.46 (0.38–0.55)	0.6 (0.44–0.65)	0.04*
Kurtosis	2.8 (2–3.6)	3.9 (2.9–4.6)	1.1 (0.3–0.6)	< 0.001*
Skewness	1.7 (1.5–1.9)	2 (1.8–2.1)	1.3 (1–1.5)	< 0.001*

Categorical and continuous variables are expressed as counts and percentage or median, with corresponding 95% confidence interval (95% CI) in parentheses. Significant P values are identified by asterisks

COVID-19, coronavirus disease 2019; *CT*, computed tomography; *HAA*, high attenuation area; *HU*, Hounsfield units; *LAA*, low attenuation area

− 700 > 35% assessed by software, the presence of exudative consolidations, the visual coronary artery calcium score > 1, and the overlap of COVID-19 CT features with other disease are independent predictors of mortality in patients affected by COVID-19. In addition, models containing quantitative and qualitative CT features assessed both visually and by open-source software showed a significant better performance in predicting mortality as compared to the clinical model.

Other imaging techniques have been advocated as predictors of death in COVID-19 pneumonia [25–27]. The evaluation of COVID-19 pneumonia extent at chest x-ray has been demonstrated as predictor of in-hospital mortality [25]. However, the predictive model including chest x-ray score, age, and immunosuppression showed lower predictive power as compared to the model based on qualitative and quantitative chest CT associated with clinical parameters displayed in the present study (AUC 0.802–0.853 vs 0.911–0.913) [25]. Higher LUS score has been reported as predictor of 30-day mortality, with lower power (AUC 0.76) compared to our predictive model containing CT parameters [26]. Furthermore, in another report, LUS assessment of COVID-19 pneumonia extent failed to identify patients with shorter survival when applied in casualty by around 40 emergency physicians on a population with disease prevalence of around

Table 3 Cox proportional-hazards regression analysis for the association of demographics, clinical, laboratory, and computed tomography features at admission to predict death (n = 248)

	Univariable analysis		Multivariable analysis					
			Clinical variables		Clinical and visual CT variables		Clinical, visual CT, and software-based variables	
Variable	Hazard ratio (95% CI)	*P* value	Hazard ratio (95% CI)	*P* value	Hazard ratio (95% CI)	*P* value	Hazard ratio (95% CI)	*P* value
Male gender (female as reference)	0.98 (0.61–1.59)	0.96	-	-	-	-	-	-
Age > 69 years old	8.91 (4.82–16.46)	< 0.001*	5.11 (2.52–10.38)	< 0.001*	3.37 (1.61–7.05)	< 0.001*	3.71 (1.79–7.7)	< 0.001*
Exposure to subject with known COVID-19	0.6 (0.36–1.004)	0.11	-	-	-	-	-	-
Comorbidities								
• Cardiovascular	2.91 (1.75–4.83)	< 0.001*	-	NS	2.25 (1.2–4.21)	0.01*	1.98 (1.07–3.66)	0.03*
• Oncological	2.66 (1.59–4.46)	< 0.001*	-	NS	2.4 (1.24–4.65)	< 0.001*	2.49 (1.3–4.77)	< 0.01*
• Neurological	3.8 (2.34–6.14)	< 0.001*	2.42 (1.41–4.16)	< 0.01*	1.74 (0.97–3.1)	0.06	-	NS
Symptoms onset ≤ 2 days	3.06 (1.87–5.03)	< 0.001*	-	NS	-	NS	-	NS
White blood cell count > $7 \times 10^3/\mu l$	2.56 (1.62–4.04)	< 0.001*	-	NS	-	NS	-	NS
CRP > 11 mg/dl	3.44 (2.17–5.46)	< 0.001*	3.07 (1.8–5.25)	< 0.001*	2.74 (1.5–5)	< 0.001*	2.65 (1.5–4.69)	< 0.001*
Blood urea > 55 mg/dl	4.77 (2.98–7.6)	< 0.001*	2.15 (1.27–3.65)	< 0.01*	-	NS	-	NS
Overall pneumonia extent visual score > 40%	3.77 (2.41–5.9)	< 0.001*	-	-	2.15 (1.2–3.85)	0.01*	-	-
Visual ground glass and crazy paving opacities extent > 40%	3.65 (2.29–5.81)	< 0.001*	-	-	-	NS	-	-
Visual consolidations extent > 10%	2.2 (1.41–3.45)	< 0.001*	-	-	-	NS	-	-
Consolidations			-	-				
• Exudative	2.06 (1.3–3.28)	< 0.01*	-	-	2.93 (1.66–5.16)	< 0.001*	2.85 (1.61–5.05)	< 0.001*
• Band-like	0.33 (0.16–0.66)	< 0.01*	-	-	-	NS	-	NS
Pleural effusion	2.34 (1.47–3.72)	< 0.001*	-	-	-	NS	-	NS
Sparing of central interstitium	0.22 (0.08–0.6)	< 0.01*	-	-	-	NS	-	NS
Visual coronary artery calcium score > 1	3.5 (2.11–5.81)	< 0.001*	-	-	2.76 (1.4–5.45)	< 0.01*	3.32 (1.71–6.46)	< 0.001*
CT categories for COVID-19								
• COVID-19 and other disease	5.10 (2.99–8.67)	< 0.001*	-	-	2.03 (1.06–3.9)	0.03*	1.92 (1–3.67)	0.04*
HAA − 700 HU > 35%	3.77 (2.39–5.97)	< 0.001*	-	-	-	-	2.17 (1.2–3.94)	0.01*
HAA − 250 HU > 5%	3.01 (1.89–4.77)	< 0.001*	-	-	-	-	-	NS
HAA − 700–250 HU > 28%	3.16 (2.01–4.97)	< 0.001*	-	-	-	-	-	NS
LAA − 950 HU > 0.3%	1.44 (0.96–2.86)	0.12	-	-	-	-	-	-
Kurtosis < 1.5	3.2 (2.1–5.03)	< 0.001*	-	-	-	-	-	NS
Skewness ≤ 1.5	3.12 (1.97–4.93)	< 0.001*	-	-	-	-	-	NS

Significant *P* values are identified by asterisks

CI, confidence interval; *COVID-19*, coronavirus disease 2019; *CRP*, C-reactive protein; *CT*, computed tomography; *HAA*, high attenuation area; *HU*, Hounsfield units; *LAA*, low attenuation area

45% [27]. Thus, qualitative and quantitative chest CT assessment in association with clinical data could be considered the best tool for the stratification of mortality risk; chest x-ray could be used as a reliable alternative in order to contain CT number while LUS should be performed by trained physician and reserved for critically ill patients when transport in the CT room is difficult.

The thresholds of CT density used to define overall pneumonia, the sum of ground-glass and crazy paving, and consolidation extent were identified by calculating a correlation coefficient among visual assessment and several thresholds obtained by the software-based histogram analysis. The %HAA − 700, %HAA − 700–250, and %HAA − 250 showed the highest correlation with overall pneumonia, the sum of ground-glass opacity and crazy-paving pattern, and consolidation extent, respectively. Similar density thresholds were used by Liu et al., who demonstrated that CT features extensions were significant predictors of progression to severe illness in COVID-19 pneumonia [7].

Overall pneumonia extent assessed visually was demonstrated as a predictor worse outcome in COVID-19 [4, 5, 10, 28]. As expected, a visual overall pneumonia extent greater than 40% was identified as predictor of mortality in the present study, higher than the threshold of around 30% reported in previous study that predicted a different composite outcome that included intensive care unit (ICU) admission or intubation and death [10, 28]. Furthermore, in the present study, the outcome was specific death for COVID-19 and not generic death, as analyzed in previous reports [10, 28].

The software-based CT assessment derived from the histogram analysis identified the %HAA − 700 higher than 35% as predictor of mortality in COVID-19. In combined pulmonary fibrosis and emphysema (CPFE), the %HAA − 700 was considered a marker of the interstitial abnormalities extent and was reported as the best predictor of diffusing capacity of the lung for carbon monoxide (DLCO) [29]. Yin et al. quantified pneumonia volume by visual segmentation using the identical open-source software and demonstrated an higher overall pneumonia extent in severe and critical COVID-19 patients [30]. To our knowledge, this is the first study that found a significant association between %HAA − 700 and mortality in COVID-19. This represents a relatively simple approach, which is warranted by open-source software widely applied in research experiments, within and beyond thoracic imaging.

Similar to previous study, the incidence at CT of COVID-19 features and other disease findings was around of 10% [16]. In the present series, an overlap between COVID-19 and other disease was demonstrated as predictor of mortality. The majority of the non-survivors patients with other disease overlap manifested signs of pulmonary edema (67%) or pneumonia other than COVID-19 (33%). Association between mortality and other concomitant diseases was reported in previous studies [31, 32]. Acute myocardial injury was demonstrated as predictor of mortality, while secondary bacterial infection occurred in 50% of COVID-19 patients who died [31, 32]. Age, COVID-19 infection, lung disease, and hearth failure were named "The Deadly Quartet" and explained the high mortality in the Northern Italy population [33]. Furthermore, 78% of the patients who underwent cardiac magnetic resonance after COVID-19 infection showed myocardial inflammation or myo-pericarditis, which have been strongly linked with adverse outcome [34, 35].

The presence of consolidations at CT was more common in patients who died than in survivors [6, 28, 32, 36]. However, the association of consolidations type and outcome was never considered in literature. We demonstrated an association between mortality and exudative consolidations that could represent bacterial concomitant infection or an evolution to adult respiratory distress syndrome (ARDS), which are associated with death in COVID-19 patients [32].

A visual coronary artery calcium score higher than 1 was demonstrated as a predictor of mortality. Ferrante et al. demonstrated that patients with COVID-19 complicated by acute myocardial injury had higher CAC score measured by

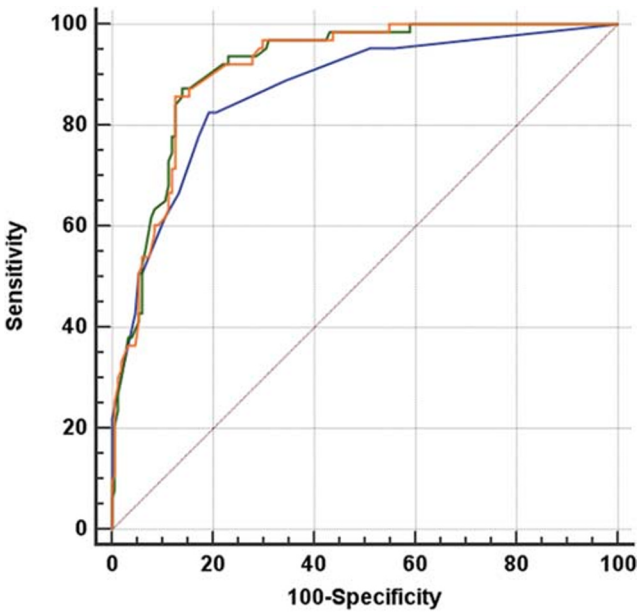

Fig. 3 Graph shows diagnostic performance in predicting death for patients with COVID-19 based on baseline clinical parameters and both qualitative and quantitative chest CT assessed visually or by open-source software. ROC curves of the models based on clinical parameters, clinical parameters and visual CT assessment, visual and software-based CT assessment added to clinical parameters are displayed respectively in blue, orange, and green lines. The AUC for the clinical model was 0.869 (95% CI 0.816–0.922). Models including clinical parameters plus both visual CT assessment (AUC 0.911, 95% CI 0.873–0.95) and visual added to software-based CT evaluation (AUC 0.913, 95% CI 0.875–0.952) showed better performance in predicting mortality (P = 0.04). AUC, area under the ROC curve; COVID-19, coronavirus disease 2019; CT, computed tomography; ROC, receiver operating characteristics

Agatston scoring system; however, CAC score failed to identify patients with higher risk of mortality [37]. This discrepancy could be explained by the different system of quantification used in the present study, based on visual assessment and not on the semi-automated Agatston system [15].

The present study has several limitations. First, it is retrospective, derived from a single center, and therefore affected by recall bias. Second, several laboratory findings such as peripheral oxygen saturation (SpO_2) and D-dimer levels were not included in the analysis. However, SpO_2 value at admission is affected by the oxygen administration time in the emergency room, which is not measurable due to the retrospective design of the study; D-dimer levels were not tested during the early outbreak, since in the inclusion period of the study, its value as predictor of worse outcome was not been yet demonstrated. Third, treatment details were not included in the survival analysis. Nevertheless, at the inclusion time of the study, no specific therapy protocol was demonstrated effective in COVID-19.

In conclusion, qualitative and quantitative chest CT parameters obtained visually or by open-source software are predictors of specific mortality in COVID-19 patients. The predictive models of mortality that included CT metrics showed better performance than clinical model in COVID-19 patients during the early outbreak.

Acknowledgments The Authors would like to thank Dr. Fausto Rapacioli for the support provided in the process of data acquisition.

The Authors thank all the doctors and nurses of their hospital for the help and energy to face such a difficult public health crisis.

Authors' contributions All authors contributed to the study conception and design. Material preparation, data collection, and analysis were performed by Davide Colombi, Gabriele D. Villani, Gabriele Maffi, Camilla Risoli, Marcello Petrini, and Mario Silva. The first draft of the manuscript was written by Davide Colombi and all authors commented on previous versions of the manuscript. All authors read and approved the final manuscript.

Data availability The datasets generated during and/or analyzed during the current study are available from the corresponding author.

Compliance with ethical standards

Conflict of interest The authors declare that they have no conflict of interest.

Ethics approval This retrospective study was approved by the Local Ethics Committee (institutional review board -IRB- approval number 582/2020/OSS*/AUSLPC). This study was performed in line with the principles of the Declaration of Helsinki. Approval was granted by the Ethics Committee of the "Area Vasta XXXXXX XXXX" (No. 582/2020/OSS*/XXXXXX)

Consent to participate The informed consent was waived by the IRB due to the retrospective nature of the study.

Consent for publication The authors affirm that human research participant provided informed consent for publication of the images in Fig. 2.

Code availability Open-source 3D Slicer software (version 4.10.2, https://www.slicer.org) with the Chest Imaging Platform application (Applied Chest Imaging Laboratory; Boston, MA, USA).

References

1. Zhu N, Zhang D, Wang W, Li X, Yang B, Song J, Zhao X, Huang B, Shi W, Lu R, Niu P, Zhan F, Ma X, Wang D, Xu W, Wu G, Gao GF, Tan W (2020) A novel coronavirus from patients with pneumonia in China, 2019. N Engl J Med 382:727–733. https://doi.org/10.1056/NEJMoa2001017
2. World Health Organization. https://covid19.who.int/?gclid=CjwKCAjw0_T4BRBlEiwAwoEiAW7pjLqt2R1sX2-3bSqkFtK27ne_nhUUSo9yiFdZIgG_5T2YYLG-SBoCuK4QAvD_BwE. Accessed 10 Aug 2020
3. Kim L, Garg S, O'Halloran A, Whitaker M, Pham H, Anderson EJ, Armistead I, Bennett NM, Billing L, Como-Sabetti K, Hill M, Kim S, Monroe ML, Muse A, Reingold AL, Schaffner W, Sutton M, Talbot HK, Torres SM, Yousey-Hindes K, Holstein R, Cummings C, Brammer L, Hall AJ, Fry AM, Langley GE (2020) Risk factors for intensive care unit admission and in-hospital mortality among hospitalized adults identified through the U.S. Coronavirus Disease 2019 (COVID-19)-Associated Hospitalization Surveillance Network (COVID-NET). Clin Infect Dis 2019:1–27. https://doi.org/10.1093/cid/ciaa1012
4. Francone M, Iafrate F, Masci GM, Coco S, Cilia F, Manganaro L, Panebianco V, Andreoli C, Colaiacomo MC, Zingaropoli MA, Ciardi MR, Mastroianni CM, Pugliese F, Alessandri F, Turriziani O, Ricci P, Catalano C (2020) Chest CT score in COVID-19 patients: correlation with disease severity and short-term prognosis. Eur Radiol. https://doi.org/10.1007/s00330-020-07033-y
5. Pan F, Zheng C, Ye T, Li L, Liu D, Li L, Hesketh RL, Yang L (2020) Different computed tomography patterns of coronavirus disease 2019 (COVID-19) between survivors and non-survivors. Sci Rep 10:11336. https://doi.org/10.1038/s41598-020-68057-4
6. Yuan M, Yin W, Tao Z, Tan W, Hu Y (2020) Association of radiologic findings with mortality of patients infected with 2019 novel coronavirus in Wuhan, China. PLoS One 15:1–10. https://doi.org/10.1371/journal.pone.0230548
7. Liu F, Zhang Q, Huang C, Shi C, Wang L, Shi N, Fang C, Shan F, Mei X, Shi J, Song F, Yang Z, Ding Z, Su X, Lu H, Zhu T, Zhang Z, Shi L, Shi Y (2020) CT quantification of pneumonia lesions in early days predicts progression to severe illness in a cohort of COVID-19 patients. Theranostics 10:5613–5622. https://doi.org/10.7150/thno.45985
8. Sun D, Li X, Guo D, Wu L, Chen T, Fang Z, Chen L, Zeng W, Yang R (2020) Ct quantitative analysis and its relationship with clinical features for assessing the severity of patients with COVID-19. Korean J Radiol 21:859–868. https://doi.org/10.3348/kjr.2020.0293
9. Rubin GD, Haramati LB, Kanne JP, Schluger NW, Yim J-J, Anderson DJ, Altes T, Desai SR, Goo JM, Inoue Y, Luo F, Prokop M, Richeldi L, Tomiyama N, Leung AN, Ryerson CJ, Sverzellati N, Raoof S, Volpi A, Martin IBK, Kong C, Bush A, Goldin J, Humbert M, Kauczor H-U, Mazzone PJ, Remy-Jardin M, Schaefer-Prokop CM, Wells AU (2020) The role of chest imaging in patient management during the COVID-19 pandemic: a multinational consensus statement from the Fleischner Society. Radiology 201365:172–180. https://doi.org/10.1148/radiol.2020201365
10. Colombi D, Bodini FC, Petrini M, Maffi G, Morelli N, Milanese G, Silva M, Sverzellati N, Michieletti E (2020) Well-aerated lung on admitting chest CT to predict adverse outcome in COVID-19 pneumonia. Radiology 296(2):E86–E96. https://doi.org/10.1148/radiol.2020201433

11. Kampf G, Todt D, Pfaender S, Steinmann E (2020) Persistence of coronaviruses on inanimate surfaces and their inactivation with biocidal agents. J Hosp Infect 104:246–251. https://doi.org/10.1016/j.jhin.2020.01.022
12. Hansell DM, Bankier AA, MacMahon H, McLoud TC, Müller NL, Remy J (2008) Fleischner Society: glossary of terms for thoracic imaging. Radiology 246:697–722. https://doi.org/10.1148/radiol.2462070712
13. Roberton BJ, Hansell DM (2011) Organizing pneumonia: a kaleidoscope of concepts and morphologies. Eur Radiol 21:2244–2254. https://doi.org/10.1007/s00330-011-2191-6
14. Ciccarese F, Coppola F, Spinelli D, Galletta GL, Lucidi V, Paccapelo A, De Benedittis C, Balacchi C, Golfieri R (2020) Diagnostic accuracy of North America Expert Consensus Statement on reporting ct findings in patients with suspected COVID-19 infection: an Italian single center experience. Radiol Cardiothorac Imaging 2:e200312. https://doi.org/10.1148/ryct.2020200312
15. Azour L, Kadoch MA, Ward TJ, Eber CD, Jacobi AH (2017) Estimation of cardiovascular risk on routine chest CT: Ordinal coronary artery calcium scoring as an accurate predictor of Agatston score ranges. J Cardiovasc Comput Tomogr 11:8–15. https://doi.org/10.1016/j.jcct.2016.10.001
16. Sverzellati N, Milanese G, Milone F, Balbi M, Ledda RE, Silva M (2020) Integrated radiologic algorithm for COVID-19 pandemic. J Thorac Imaging 35:228–233. https://doi.org/10.1097/RTI.0000000000000516
17. Ichikado K, Muranaka H, Gushima Y, Kotani T, Nader HM, Fujimoto K, Johkoh T, Iwamoto N, Kawamura K, Nagano J, Fukuda K, Hirata N, Yoshinaga T, Ichiyasu H, Tsumura S, Kohrogi H, Kawaguchi A, Yoshioka M, Sakuma T, Suga M (2012) Fibroproliferative changes on high-resolution CT in the acute respiratory distress syndrome predict mortality and ventilator dependency: a prospective observational cohort study. BMJ Open 2:1–11. https://doi.org/10.1136/bmjopen-2011-000545
18. Edey AJ, Devaraj AA, Barker RP, Nicholson AG, Wells AU, Hansell DM (2011) Fibrotic idiopathic interstitial pneumonias: HRCT findings that predict mortality. Eur Radiol 21:1586–1593. https://doi.org/10.1007/s00330-011-2098-2
19. Fedorov A, Beichel R, Kalpathy-Cramer J, Finet J, Fillion-Robin J-C, Pujol S, Bauer C, Jennings D, Fennessy F, Sonka M, Buatti J, Aylward S, Miller JV, Pieper S, Kikinis R (2012) 3D Slicer as an image computing platform for the Quantitative Imaging Network. Magn Reson Imaging 30:1323–1341. https://doi.org/10.1016/j.mri.2012.05.001
20. Cohen J (1968) Weighted kappa: nominal scale agreement with provision for scaled disagreement or partial credit. Psychol Bull 70:213–220. https://doi.org/10.1037/h0026256
21. Koo TK, Li MY (2016) A guideline of selecting and reporting intraclass correlation coefficients for reliability research. J Chiropr Med 15:155–163. https://doi.org/10.1016/j.jcm.2016.02.012
22. McHugh ML (2012) Interrater reliability: the kappa statistic. Biochem Med (Zagreb) 22(3):276–282
23. World Health Orginization (2020) International guidelines for certification and classification (coding) of COVID-19 as cause of death: based on ICD. Int Stat Classif Dis 3
24. DeLong ER, DeLong DM, Clarke-Pearson DL (1988) Comparing the areas under two or more correlated receiver operating characteristic curves: a nonparametric approach. Biometrics 44:837–845
25. Borghesi A, Zigliani A, Golemi S, Carapella N, Maculotti P, Farina D, Maroldi R (2020) Chest X-ray severity index as a predictor of in-hospital mortality in coronavirus disease 2019: a study of 302 patients from Italy. Int J Infect Dis 96:291–293. https://doi.org/10.1016/j.ijid.2020.05.021
26. Lichter Y, Topilsky Y, Taieb P, Banai A, Hochstadt A, Merdler I, Gal Oz A, Vine J, Goren O, Cohen B, Sapir O, Granot Y, Mann T, Friedman S, Angel Y, Adi N, Laufer-Perl M, Ingbir M, Arbel Y, Matot I, Szekely Y (2020) Lung ultrasound predicts clinical course and outcomes in COVID-19 patients. Intensive Care Med 46:1873–1883. https://doi.org/10.1007/s00134-020-06212-1
27. Colombi D, Petrini M, Maffi G, Villani GD, Bodini FC, Morelli N, Milanese G, Silva M, Sverzellati N, Michieletti E (2020) Comparison of admission chest computed tomography and lung ultrasound performance for diagnosis of COVID-19 pneumonia in populations with different disease prevalence. Eur J Radiol 133:109344. https://doi.org/10.1016/j.ejrad.2020.109344
28. Guillo E, Bedmar Gomez I, Dangeard S, Bennani S, Saab I, Tordjman M, Jilet L, Chassagnon G, Revel MP (2020) COVID-19 pneumonia: diagnostic and prognostic role of CT based on a retrospective analysis of 214 consecutive patients from Paris, France. Eur J Radiol 131:109209. https://doi.org/10.1016/j.ejrad.2020.109209
29. Matsuoka S, Yamashiro T, Matsushita S, Kotoku A, Fujikawa A, Yagihashi K, Nakajima Y (2015) Quantitative CT evaluation in patients with combined pulmonary fibrosis and emphysema: correlation with pulmonary function. Acad Radiol 22:626–631. https://doi.org/10.1016/j.acra.2015.01.008
30. Yin X, Min X, Nan Y, Feng Z, Li B, Cai W, Xi X, Wang L (2020) Assessment of the severity of coronavirus disease: quantitative computed tomography parameters versus semiquantitative visual score. Korean J Radiol 21:1–9. https://doi.org/10.3348/kjr.2020.0423
31. Chen FZMLYZYZKSDMXZY (2020) The characteristics and outcomes of 681 severe cases with COVID-19 in China. J Crit Care 60:32–37. https://doi.org/10.1016/j.jcrc.2020.07.003
32. Zhou F, Yu T, Du R, Fan G, Liu Y, Liu Z, Xiang J, Wang Y, Song B, Gu X, Guan L, Wei Y, Li H, Wu X, Xu J, Tu S, Zhang Y, Chen H, Cao B (2020) Clinical course and risk factors for mortality of adult inpatients with COVID-19 in Wuhan, China: a retrospective cohort study. Lancet 395:1054–1062. https://doi.org/10.1016/S0140-6736(20)30566-3
33. Calcaterra G, Bassareo PP, Barilla F, Sergi D, Chiocchi M, Romeo F, Mehta JL (2020) The Deadly Quartet (Covid-19, old age, lung disease, and heart failure) explain why coronavirus-related mortality in northern Italy was so high. Curr Cardiol Rev. https://doi.org/10.2174/1573403X16666200731162614
34. Puntmann VO, Carerj ML, Wieters I, Fahim M, Arendt C, Hoffmann J, Shchendrygina A, Escher F, Vasa-Nicotera M, Zeiher AM, Vehreschild M, Nagel E (2019) Outcomes of cardiovascular magnetic resonance imaging in patients recently recovered from coronavirus disease 2019 (COVID-19). JAMA Cardiol 2020:1–9. https://doi.org/10.1001/jamacardio.2020.3557
35. Puntmann VO, Carr-White G, Jabbour A, Yu CY, Gebker R, Kelle S, Hinojar R, Doltra A, Varma N, Child N, Rogers T, Suna G, Arroyo Ucar E, Goodman B, Khan S, Dabir D, Herrmann E, Zeiher AM, Nagel E (2016) T1-mapping and outcome in nonischemic cardiomyopathy all-cause mortality and heart failure. JACC Cardiovasc Imaging 9:40–50. https://doi.org/10.1016/j.jcmg.2015.12.001
36. Li Y, Yang Z, Ai T, Wu S (2019) Xia L (2020) Association of "initial CT" findings with mortality in older patients with coronavirus disease 2019 (COVID-19). Eur Radiol 30:6186–6193. https://doi.org/10.1007/s00330-020-06969-5
37. Ferrante G, Fazzari F, Cozzi O, Maurina M, Bragato R, D'Orazio F, Torrisi C, Lanza E, Indolfi E, Donghi V, Mantovani R, Liccardo G, Voza A, Azzolini E, Balzarini L, Reimers B, Stefanini GG, Condorelli G, Monti L (2020) Risk factors for myocardial injury and death in patients with COVID-19: insights from a cohort study with chest computed tomography. Cardiovasc Res. https://doi.org/10.1093/cvr/cvaa193